

Cellular senescence affects energy metabolism, immune infiltration and immunotherapeutic response in Hepatocellular Carcinoma

Biao Gao

Faculty of Hepato-Pancreato-Biliary Surgery Chinese PLA General Hospital

Shichun Lu (✉ lusc_301@163.com)

Faculty of Hepato-Pancreato-Biliary Surgery Chinese PLA General Hospital

Research Article

Keywords: Cellular senescence, Hepatocellular carcinoma, Energy metabolism, Chemokines, Immunotherapy, Predictive Models

Posted Date: May 19th, 2022

DOI: <https://doi.org/10.21203/rs.3.rs-1642647/v1>

License:   This work is licensed under a Creative Commons Attribution 4.0 International License.

[Read Full License](#)

Abstract

Background Aging is an inevitable consequence of life, characterized by a progressive decline in tissue and organ function and an increased risk of death. There is growing evidence that aging is closely related to tumor development and immune regulation. However, in hepatocellular carcinoma, the relationship between cellular senescence and immune infiltration, energy metabolism, chemokines, and immunotherapeutic response is unclear and needs further study.

Methods: We first analyzed 274 cellular senescence-associated genes by the NMF algorithm and identified two cellular senescence-associated clusters. Subsequently, we compared the differences between the two clusters, in terms of immune infiltration, energy metabolism, chemokines, and immunotherapeutic response to treatment. We further constructed risk models using cellular senescence-associated signature genes that could effectively identify the two subpopulations. Finally, we validated the validity and robustness of the risk model using an external dataset.

Results: We found significant differences in survival prognosis between two cellular senescence-associated clusters. In addition, we found significant differences in immune cell infiltration, expression of energy metabolism-related genes, expression of chemokine-related genes, expression of immune checkpoint-related genes, Tumor Immune Dysfunction and Exclusion between the two clusters. Also, a scoring system associated with cellular senescence was developed and validated as an independent prognostic indicator. It was validated as an independent prognostic factor and immunotherapeutic predictor for HCC. The cellular senescence-related scoring system was validated as an independent prognostic factor and immunotherapy predictor for HCC, and patients with low CSS were characterized by prolonged survival time.

Conclusion: Our study confirmed the relationship between cellular senescence and immune cell infiltration, energy metabolism, chemokines, expression of immune checkpoint-related genes, and response to immunotherapy. This enhances our understanding of cellular senescence and tumor immune microenvironment, energy metabolism, chemokines, and provides new insights to improve immunotherapy outcomes in HCC patients. It provides new insights to improve the outcome of immunotherapy in HCC patients.

Introduction

Hepatocellular carcinoma (HCC) is a global health problem with increasing incidence and mortality^[1, 2]. Despite the increasing use of surgical and local treatments worldwide^[3], it is estimated that about 50-60% of HCC patients will eventually undergo systemic therapy^[4]. Since 2017, immunotherapy has been another major breakthrough in advanced HCC with encouraging results. In recent years, with this single-cell and second-generation sequencing, multi-omics research, bioinformatics and tumor microenvironment (TME) research, biomarkers including gene alterations and pathway activations are of

great significance for designing proper treatment regimens, and biomarker-driven therapies have shown gratifying benefits^[5]. Targeted therapy, immune checkpoint suppression therapy, and combination therapy of HCC have shown superior efficacy in clinical trials. Although the understanding of HCC genomics and breakthroughs in targeted therapy and immunotherapy have greatly expanded the treatment paradigm. Breakthroughs in targeted therapies and immunotherapy have expanded the HCC treatment paradigm. The challenges associated with HCC remain elusive. For example, most HCC patients have a low response rate to immunotherapy of 15-25%^[6], which falls far short of clinical needs. Currently, even though the objective response rate of immune checkpoint blockers (ICB) has almost doubled in combination with targeted drug therapy, more than half of the patients still do not respond^[7]. In addition, ICB can cause serious immune-related adverse events and a new pattern of excessive progression (accelerated tumor growth) during PD-1/PD-L1-targeted therapy (8% of cases in HCC)^[8, 9]. Biomarker-based patient selection can help maximize efficacy and reduce the number of patients who may not benefit or even be harmed by ICB.

Therefore, better immunotherapy prediction tools and biomarkers that accurately predict tumor characteristics are urgently needed to stratify patients and personalize treatment for HCC.

Cellular senescence is a complex stress response that affects cellular function and organismal health. Multiple developmental and environmental factors, such as radiation, oxidative stress, oncogenes and protein accumulation, activate genes and pathways leading to senescence^[10]. Regardless of the stimuli, senescent cells share some common behaviors, among which the main ones are growth arrest, apoptosis resistance, sustained DNA damage signaling, and heterochromatin modifications^[11]. A growing body of research suggests that aging accompanies cellular senescence and that by manipulating the biological process of cellular senescence can slow or retard many diseases associated with aging, such as cancer^[12, 13]. Recent studies have confirmed that aging and cellular senescence affect the immune microenvironment (TME) by promoting the accumulation of multiple types of immunosuppressive cells and activating various risk-related signaling molecules and cytokines, which have a broad impact on the TME and tumor growth^[14, 15]. At the same time, cellular senescence changes the adaptability of immune cells in the TME, thus altering the efficacy of tumor immunotherapy to some extent^[16, 17]. Therefore, an improved understanding of the impact of senescence on tumor immunity associated with invasion and development is required to frame novel treatment paradigms for tumors.

To provide a comprehensive and systematic understanding of the relationship between cellular senescence and immune infiltration, energy metabolism, chemokines, and immunotherapy response in HCC, we established a novel risk model based on cellular senescence-related genes and explored their potential importance as predictive biomarkers for prognosis and immunotherapy response. We further explored the mechanisms by which tumor cell senescence-associated genes affect the TME. Subsequently, we validated the robustness and validity of cellular senescence-related prediction models in an external dataset. This study provided new insights into the regulatory mechanisms of cellular senescence associated with the TME and strategies for HCC immunotherapy.

Materials And Methods

Data and Clinical Samples

We collected gene expression data and complete clinical information data from 424 HCC patients using The Cancer Genome Atlas (TCGA,

<https://portal.gdc.cancer.gov/>), which contains 365 tumor tissues and 59 normal tissue samples, as a training set. Similarly, to validate the robustness of the model, we downloaded the sample information of tumor tissues from 240 HCC patients from ICGC(<https://dcc.icgc.org/>) as the validation set. The clinical features of the 365 liver cancer patients included in the training set are summarized in Table I. The 279 cellular senescence-associated genes in this study were obtained from the CellAge database (<https://genomics.senescence.info/cells/>), which contains manually managed human gene data associated with cellular senescence.

Table 1

Clinical characteristics of 365 HCC patients in TCGA

Characteristics	Samples(n=365)	Percentage(%)
Gender		
Female	120	32.9%
Male	245	67.1%
Age		
>=60	200	54.8%
<60	165	45.2%
T		
T1	180	49.3%
T2	91	25.0%
T3	81	22.2%
T4	13	3.6%
M		
M0	263	72.1%
MX	102	28.0%
N		
N0	248	67.9%
N1	5	1.4%
NX	112	30.7%
Grade		
G1	58	15.9%
G2	176	48.2%
G3	116	31.8%
G4	13	3.6%

Identification of cellular senescence clusters by NMF

We used the "non-negative matrix factorization (NMF) clustering algorithm of the NMF package of R software

algorithm to cluster 365 HCC samples based on the expression levels of 279 cellular senescence-related genes to identify distinct cellular senescence clusters. The "brunet" option was selected and 100 iterations were performed for the NMF. We determined the optimal number of clusters based on the apparent coefficients, dispersion coefficients and silhouette coefficients to determine the optimal number of clusters for the 365 HCC samples.

Differences between clinical features

We further investigated the relationship between the clusters obtained by NMF clustering and clinical characteristics to determine the effects of cellular aging-related and genes on clinical characteristics.

Differentially expressed genes (DEGs) and Functional enrichment analysis

We used the "limma" package of the R software to perform differential analysis of the different clusters with the screening criteria of $pvalue < 0.05$ and $logFC > 2$ or $logFC < -2$. To further investigate the differences in molecular mechanisms between different clusters, we used the "clusterProfiler" package of R software to perform functional enrichment analysis of up-regulated and down-regulated genes separately, with $P < 0.05$ considered statistically significant.

Differences between chemokines, energy metabolism between different clusters

The Molecular Signature Database (MSigDB, <http://www.broad.mit.edu/gsea/msigdb/>) was utilized to contain two energy metabolism-related gene sets (energy-requiring part of metabolism and reactome energy metabolism). We further downloaded the chemokine-related gene set from TISIDB (<http://cis.hku.hk/TISIDB/>). To further investigate the relationship between cellular senescence and chemokines and energy metabolism, we compared the expression of chemokines and energy metabolism-related genes among different clusters.

Evaluation of immune infiltration between different clusters

CIBERSORT is a deconvolution technique that utilizes RNA-Seq data to determine the makeup of immune cells. We used CIBERSORT to analyze RNA expression data from 365 HCC samples, thus comparing the differences between different clusters in terms of immune infiltrating cells. Meanwhile single sample gene set enrichment analysis (ssGSEA) was implemented to estimate immune cell abundance of each sample in TCGA cohort based on a gene panel marking 28 immune cell types. We further compared the differences between different clusters in intratumor heterogeneity (ITH), SNV neoantigen, CTA scores, Homologous Recombination Defects (HRD). We further analyzed the RNA expression information of 365 HCC cases using the ESTIMATE function of R software to evaluate the differences between different clusters in StromalScore, ImmuneScore, ESTIMATEScore, TumorPurity.

Differences in tumor mutation and immune checkpoint-associated gene expression among clusters

We downloaded somatic mutation data from TCGA for all HCC samples and used the maftools package of R software to analyze different clusters and thus compare differences between clusters in terms of gene mutation and tumor mutation load (TMB). (TMB = (total mutations/total number of tests) *10⁶). We further compared the differences in expression of immune checkpoint-related genes, such as PD-L1, PD1, PD-L2, TIM-3, and TIGIT, among different clusters.

Prediction of immunotherapeutic response

The Tumor Immune Dysfunction and Exclusion(TIDE, <http://tide.dfci.harvard.edu/>) and immunophenotype scores(IPS, <https://tcia.at/>) , considered to be the best predictor of response to immunotherapy, was used to predict response to immunotherapy among distinct cellular senescence clusters.

Construction and validation of a cellular senescence-related scoring system

We further constructed the cellular senescence-related scoring system to better represent cellular senescence. We used the "limma" package of R (version 4.1.2) to perform differential analysis among clusters with the screening criteria of pvalue < 0.05 and logFC > 1 or logFC < -1, to obtain differential expressed genes. Univariate Cox proportional hazard regression analysis was performed to identify cellular senescence-related prognostic genes (p < 0.05). Next, the DEGs and prognostic genes were investigated using the R package "veen" to acquire prognostic cellular

senescence-related DEGs, and correlations were visualized by the R package "circlize". To eliminate overfitting, a least absolute shrinkage and selection operator (LASSO) Cox regression analysis was used in conjunction with the "glmnet" package. Finally, we utilized Cox multifactor analysis on the screened variables to find independent prognostic risk factors and construct an **cellular senescence-related scoring system**.

Risk score = expression of gene a coefficient a multiplied by expression of gene b coefficient b multiplied by expression of gene c coefficient c multiplied by expression of gene n coefficient n. Following that, all patients were classified as high-risk or low-risk based on their median risk ratings. We validated the robustness of the scoring system using the survival data of 240 HCC patients from the ICGC database.

Results

Identification of different cellular senescence-associated clusters

To comprehensively explore the expression patterns of cellular senescence-related genes in HCC, we downloaded the information of RNA sequencing samples and clinical information of 424 HCC patients from the TCGA database as the training set, and we downloaded the information of RNA sequencing samples and clinical information of 240 HCC patients from the ICGC database as the validation set. Based on the expression profiles of 281 cellular senescence-associated genes, we stratified 365 HCC

patient samples in the training set into two different clusters (233 cases in Cluster 1 (C1), 132 cases in Cluster 2 (C2) by a nonnegative matrix factorization (NMF) algorithm(Figure 1A). In the training set, the survival of C1 patients was significantly better than that of C2 patients, and the survival curves are shown in Figure 1B. Subsequently, we further compared the differences between clusters in terms of basic clinical characteristics, and we found that C2 patients had a greater proportion of HCC patients with T3 and T4 stages compared with C1 patients, while patients with Grade classification G3 and G3 were significantly more represented in C1 than in C2 (Log-rank test, $P<0.05$)(Figure 1C- Figure 1F). The above results suggest that there is a relationship between the expression of genes related to cellular senescence and clinical characteristics T stage and Grade classification.

Differential gene analysis and functional enrichment analysis

To further investigate the differences in gene expression and biological processes involved between different clusters, we further performed differential gene analysis between different clusters, in which 123 genes were up-regulated in C1 and 2253 genes were up-regulated in C2(Figure 2A- Figure 2B). The GO enrichment analysis showed that the biological process (BP) of up-regulated genes in C1 was mainly enriched in small molecule catabolic process and carboxylic acid catabolic process; the most enriched cellular component (CC) was high-density lipoprotein particle and plasma lipoprotein particle. GO enrichment analysis revealed that the biological processes (BP) of upregulated genes in C2 were mainly enriched in cellular responses to copper ions and secondary metabolic processes; the most enriched cellular components (CC) were the multivesicular body membrane and apical plasma membrane(Figure 2C- Figure 2D). KEGG functional enrichment analysis showed that in cluster1 upregulated genes were mainly enriched in Chemical carcinogenesis - DNA adducts and Metabolism of xenobiotics by cytochrome P450 pathway, while in C2 .The upregulated genes in C2 were mainly enriched in Neuroactive ligand-receptor interaction, Protein digestion and absorption pathway(Figure 2E- Figure 2F). We then performed GSEA (KEGG) enrichment on the two clusters showing that in cluster1 the DRUG_METABOLISM_CYTOCHROME_P450 pathway and RETINOL_METABOLISM pathway were mainly enriched, while in C2 the OOCYTE_MEIOSIS pathway and PROGESTERONE_MEDIATED_OOCYTE_MATURATION pathway were mainly enriched(Figure 3A). Multiple enrichment analysis revealed that C2 is mainly involved in pathways associated with cellular senescence.

Differences in chemokine and energy metabolism-related genes among clusters

We further compared the expression differences of chemokine and energy metabolism-related genes in cluster1 and C2. we found that in C2, the expression of most chemokine-related genes was significantly higher than in C1(Figure 3B), especially CCL26, CXCL5, CXCL6, CXCL1(Figure 3C- Figure 3F). similarly, the we found that most of the energy metabolism-related genes were highly expressed in C2 (Figure 4A- Figure 4G). We further enriched the differential energy metabolism-related genes, and we found that these differential frontal energy metabolism-related genes were mainly enriched in xenobiotic metabolic process, cellular response to xenobiotic stimulus, and carbohydrate biosynthetic process pathways(Figure 5A- Figure 5B).The above results further suggest that there is a link between cellular

senescence and tumor microenvironment, while cellular senescence can change the energy metabolic state to some extent.

Characterization of immune landscape in distinct cellular senescence clusters

Previous studies have demonstrated a relationship between cellular senescence and tumor immune infiltration in a variety of tumor types^[18, 19]. We calculated the proportion of 21 immune cell species in each HCC sample using the R software CIBERSORT, while comparing the differences between immune cell components across clusters (Figure 5C). Particularly, we found that regulatory T cells (Tregs) was markedly elevated in C2. Subsequently, we applied the ssGSEA algorithm to determine the relative ratios of 28 immune cells and immune-related pathways in each HCC sample, comparing the differences in immune cell composition between clusters (Figure 5D- Figure 5E). We found that most immune cells were significantly enriched in C2, and interestingly, Myeloid-derived suppressor cells (MDSCs) cells (MDSCs) were significantly higher in C2 than in C1, which was concordant with previous observations linking C2 to an immunosuppressive phenotype. We further compared the effect of infiltrating immune cells on the survival of HCC patients, and we found that patients with highly infiltrated CD8T cells, M0 Macrophages, had a better prognosis; while highly infiltrated M2 Macrophages cells had the opposite result (Figure 5F- Figure 5H). In addition, we calculated the StromalScore, ImmuneScore, ESTIMATEScore, and TumorPurity for each HCC sample using the ESTIMATE function of R software, and the ImmuneScore of C2 was significantly higher than that of C1, in agreement with the previous results (Figure 6A- Figure 6D). Overall, these results confirm that cellular senescence is associated with the tumor microenvironment, to some extent, contribute to the formation of an immunosuppressive microenvironment.

Landscape of tumor mutation and immune checkpoint-associated gene expression in different clusters

We compared the differences in somatic mutations and tumor mutational load (TMB) between clusters and showed that there was no significant difference in somatic mutation frequency and TMB between C1 and C2 (Figure 7C), interestingly, C1 had the CTNNB1 gene as the major mutated gene while C2 had the TP53 gene as the major mutated gene (Figure 7A- Figure 7B). Immunomodulators play an important role in reshaping the tumor microenvironment. Therefore, to further explore the complex communication between immunomodulators, immune infiltration and cellular senescence, we explored the expression of immune checkpoint-associated genes among different clusters. We found that most immune checkpoint-related genes, including PD-L1, PD1, PD-L2, TIM-3 were significantly upregulated in C2, further suggesting that the presence of an immunosuppressive microenvironment in C2 (Figure 6E- Figure 6H). Finally, we used the TIDE score to assess the clinical effectiveness of immunotherapy across clusters. In our results, C2 had the lower TIDE score (Figure 7D- Figure 7F), implying that patients in C2 could benefit more from immunotherapy than C1.

Taken together, our comprehensive analysis showed that cellular senescence clusters are significantly associated with energy metabolism, chemokines, tumor microenvironment and patient prognosis, which may provide new insights into HCC classification system.

Construction of the cellular senescence score for overall survival in HCC patients

In order to better reflect the characteristics of C1 and C2, we constructed a risk score model to differentiate HCC patients. First, we performed differential gene analysis for C1 and C2 with the screening criteria of $p\text{value} < 0.05$ and $\log\text{FC} > 1$ or $\log\text{FC} < -1$. A total of 8341 differential genes were obtained. Subsequently, we selected 68 genes that overlapped with the set of genes associated with cellular senescence (Figure 7G). We identified 36 prognosis-associated cellular senescence genes using Cox univariate regression analysis (Figure 7H); we then used LASSO Cox regression analysis and multifactorial Cox regression analysis to build prognostic models (Figure 8A- Figure 8C). Four prognostic genes (CENPA, CXCL8, EZH2, and G6PD) were identified in the training set used to build the prognostic model. The prognostic risk score was calculated using the following formula: $\text{risk score} = (0.22281 \times \text{CENPA gene expression}) + (0.10830 \times \text{CXCL8 gene expression}) + (0.19533 \times \text{EZH2 gene expression}) + (0.18866 \times \text{G6PD gene expression})$. Patients in the training set were divided into a high-risk group and a low-risk group based on the median risk score. Patients in the low-risk group had significantly higher postoperative survival rates than those in the high-risk group (Figure 8F). We evaluated the predictive efficacy of risk scores on the prognosis of HCC patients using ROC curves (Figure 8D- Figure 8E). We further analyzed the clinical factors with risk score and found that risk score and T-stage were independent risk factors affecting the prognosis of HCC patients (Figure 8G- Figure 8H). We used the validation set to determine the model's robustness and prognostic value. On the basis of risk scores for four genes, the validation set's 240 patients were divided into a high-risk and a low-risk group. Kaplan-Meier survival curve analysis revealed that patients in the low-risk group survived significantly longer than those in the high-risk group ($p < 0.001$) (Figure 9G- Figure 9H).

Meanwhile, we further explored the relationship between risk scores and different clusters, and we found that the high-risk score group was more responsive to the characteristics of C2; similarly, the low-risk score group responded to the characteristics of C1 (Figure 9F). Therefore, we believe that the risk score of this model can well reflect the characteristics of cellular senescence in HCC.

Construction of integrated models to optimize risk stratification and survival prediction in HCC patients

To better predict the probability of survival in HCC patients, we created a predictive nomogram based on the integration of risk scores and other clinicopathological features (Figure 9A). Age, gender, T-stage, N-stage, M-stage, and Grade stage were included. The calibration curves of the nomogram for 1, 3 and 5 year survival probabilities showed excellent agreement with the ideal performance (Figure 9B- Figure 9D). This indicates a high accuracy of our nomograms. In addition, the nomogram based on risk score showed the best ability to predict OS most strongly compared to other clinicopathological characteristics (age, gender, T stage, N stage, M stage and Grade classification) with a mean AUC higher than 0.6 (Figure 9E).

Discussion

HCC is the sixth most common cancer in the world, and it is the fourth most lethal^[20]. The introduction of immune checkpoint inhibitors in recent years has dramatically changed the treatment of hematologic and solid tumors, including HCC^[21, 22]. However, the immunotherapy of HCC has proven a challenge for the era of personalized therapy due to inter- and intra-tumoral heterogeneity. At the same time, significant problems such as low response rates to immunotherapy still exist in clinical practice, so it is crucial to use biomarkers to predict prognosis and immunotherapeutic response, and thus to implement personalized therapy for individuals.

Senescence is an injury-induced stress program that activates a series of pleiotropic cytokines, chemokines, growth factors, and proteases of the senescence-associated secretory phenotype (SASP), ultimately leading to persistent suppression of tumor cells and remodeling of the tumor immune microenvironment^[23]. A growing number of studies have confirmed that senescent cells can be removed by SASP to stimulate the immune response and thus achieve clearance^[18]. Thus, SASPs are positive for the body in the short term. However, in the long term, these functions could become detrimental in the context of immunosuppression of cancer to promote tumor development^[24-26]. However, the association and value between cellular senescence, energy metabolism, chemokines, and tumor immune infiltration have not been reported, especially in HCC. Therefore, studies on the biological mechanisms and prognostic biomarkers of HCC concerning cellular senescence-related genes may offer an opportunity to identify HCC subtypes, improving the future application of precision-focused treatments for HCC. In addition, the existing immunotherapeutic drugs suffer from both low response rate to immunotherapy, drug tolerance and failure to meet clinical needs, so revealing the immune microenvironment from the level of cellular senescence will provide new perspectives for the development of related drugs.

. With the development of second-generation sequencing technologies, transcriptome analysis has paved the way for the identification of new prognostic and predictive biomarkers to discern the heterogeneity and complexity of tumors in order to develop new, individualized treatment strategies. Based on the expression of cellular senescence-related genes, we randomly divided the 365 HCC samples in the TCGA database into C1 and C2. Interestingly, we found significant differences in immune cell infiltration, energy metabolism, and chemokines between C1 and C2. The findings suggest that cellular senescence-associated genes may contribute to different biological processes and immune phenotypes, while cellular senescence-associated genes are somehow intrinsically linked to the expression of energy metabolism and chemokine-related genes. These genes have been associated with different tumorigenesis and anti-cancer immunity of individual tumors. Cellular senescence cluster 2 is significantly enriched in cell division, tumor-related signaling pathways, including Oocyte meiosis, Cell cycle, Pathways in cancer; also associated with cellular interactions, including Neuroactive ligand-receptor interaction, Cytokine-cytokine receptor interaction. Interestingly, immune infiltrating cell analysis showed a higher percentage of MDSC, Tregs cells in cluster2, suggesting that patients in cluster2 may be associated with an immunosuppressed state. Accordingly, immune checkpoint-related genes were significantly more highly expressed in cluster2, further confirming the existence of an immunosuppressive microenvironment in

cluster2. Also, we found a lower TIDE score in cluster2, suggesting that patients in cluster2 are more likely to benefit from immunotherapy. Taken together, the newly identified cellular senescence

clusters might provide novel insights on classification system of HCC.

We constructed a novel survival prediction model based on the expression of four cellular senescence-associated genes (CENPA, IL8, EZH2, G6PD) by the stochastic survival forest method. In addition, we merged survival prediction models with clinical characteristic factors and constructed Nomograms as a way to quantify risk scores and survival probabilities. Compared with other traditional predictors, the prediction models based on cellular senescence-related genes showed better accuracy and discriminatory performance in survival prediction. Notably, our results imply that risk score is an independent prognostic factor for HCC patients and also a predictor of immunotherapy. It has been suggested that a high risk score may be associated with a favorable response to ICI treatment.

Risk scores coupled with specific immune checkpoint factors may serve as predictive biomarkers of ICI response and prognosis.

All four associated genes of our cellular senescence-associated gene model have been demonstrated in a variety of tumors. For example, a report by Li et al. found that CENPA overexpression was associated with advanced histological grade, positive serum HBsAg status, Ki-67 expression, and p53 immunopositivity^[27]. Shabangu's study showed that persistent high levels of HCV can induce altered cell adhesion and migration-promoting gene expression through the CXCL8-SRC signaling pathway^[28]. A study by Na Bae et al^[29]. concluded that overexpression of EZH2 was significantly associated with poorer prognosis in HCC patients and that EZH2 could be a potential target for HCC immunotherapy. Lu et al^[30]. found that G6PD induces epithelial-mesenchymal transition through activation of signal transducer and activator of transcription 3 (STAT3) pathway, which contributes to HCC migration and invasion of hepatocellular carcinoma cells.

Overall, our study provides important implications for clinical research. First, we have developed and discovered a novel scoring system that can classify patients with different treatment strategies based on different risk subgroups. We found that the risk score correlated with immune cell infiltration in TME, with more immune cell infiltration in the high-risk group, but also a higher proportion of immunosuppressive cells such as MDSC, Tregs cells, suggesting an immunosuppressive state in HCC patients with high risk scores. In addition, we found that HCC patients in the high-risk group exhibited lower TIDE scores and higher expression of immune checkpoint-related genes, suggesting a possible higher response to immunotherapy. Our model showed better predictive power compared to other existing biological markers. These results suggest that cellular senescence scores may further stratify patient response to immunotherapy in HCC. thus, our study of the effect of cellular senescence on TME may enhance the understanding of immunotherapy response heterogeneity. Second, we found that cellular senescence correlated with the expression of energy metabolism and chemokine-related genes, with higher expression of energy metabolism and chemokine-related genes in HCC patients with higher risk scores,

suggesting more vigorous energy metabolism and stronger inflammatory response in senescent cells. Glycolysis is a feature of both cancer cell progression and T cell activation^[31]. Previous reports have suggested that microenvironmental glucose competition may be a driver of immunosuppression by depleting necessities required to maintain effector T cell function, whereas blockade of glycolysis in malignant cells can boost the efficiency of immunotherapy and metabolic remodeling between tumor cells and T cells^[32]. Therefore, reflecting the cellular senescence status from the perspective of tumor energy metabolism and inflammatory response will help us to have a deeper understanding of tumor cell senescence. Taken together, uncovering the relationship between tumor cell senescence and energy metabolism, TME and inflammatory responses may provide a perspective on cellular senescence from an immune, metabolic, and inflammatory perspective, allowing us to discover how to effectively reshape the immunosuppressive microenvironment by inhibiting the senescence process or destroying senescent cells, so-called anti-aging therapies.

Although, our study has value in immunotherapy and prognosis for HCC, there are certain flaws in this study. First, the four cellular senescence-associated gene sets we constructed are based on public databases, and therefore, external multicenter samples are needed for validation. Second, prospective clinical trials are necessary to verify the applicability of our findings in patients with LUAD receiving immunotherapy. Third, the regulatory mechanism of cellular senescence-associated genes on TME needs to be further confirmed in in vitro and in vivo experiments. Finally, the preliminary interpretation of mechanisms underlying the association between cellular senescence-related genes and worse response to ICIs must be further elucidated using basic experiments.

Conclusions

Finally, the cellular senescence risk profile presented in this study can be used to predict survival, identify molecular subtypes of HCC that may respond to immunotherapy, and provide a basis for clinical treatment planning. In the future, this model could provide a reliable predictive tool for HCC patients.

Declarations

Ethics approval and consent to participate

Not applicable.

Consent for publication

Not applicable.

Availability of data and materials

The 279 cellular senescence-associated genes were downloaded from the CellAge database (<https://genomics.senescence.info/cells/>). The datasets generated and analyzed during the current study

are available in the [https:// portal. gdc. cancer. gov/](https://portal.gdc.cancer.gov/) and [https:// dcc. icgc. org/ proje cts/ LIRI- JP](https://dcc.icgc.org/projects/LIRI-JP).

Competing interests

The authors declare that they have no competing interests.

Funding

This research received a grant from National Natural Science Foundation of China (No.81670590)

Author contributions

BG performed the data analysis and wrote the manuscript.SL reviewed and revised the manuscript. All authors read and approved the final manuscript.

Acknowledgements

We would like to acknowledge the TCGA, ICGC and CellAge for providing relevant data.

References

1. Sung H, Ferlay J, Siegel R L, et al. Global Cancer Statistics 2020: GLOBOCAN Estimates of Incidence and Mortality Worldwide for 36 Cancers in 185 Countries[J]. *CA Cancer J Clin*, 2021,71(3):209-249. DOI: 10.3322/caac.21660.
2. Llovet J M, Kelley R K, Villanueva A, et al. Hepatocellular carcinoma[J]. *Nat Rev Dis Primers*, 2021,7(1):6. DOI: 10.1038/s41572-020-00240-3.
3. Llovet J M, De Baere T, Kulik L, et al. Locoregional therapies in the era of molecular and immune treatments for hepatocellular carcinoma[J]. *Nat Rev Gastroenterol Hepatol*, 2021,18(5):293-313. DOI: 10.1038/s41575-020-00395-0.
4. Llovet J M, Montal R, Sia D, et al. Molecular therapies and precision medicine for hepatocellular carcinoma[J]. *Nat Rev Clin Oncol*, 2018,15(10):599-616. DOI: 10.1038/s41571-018-0073-4.
5. Ling Y, Liu J, Qian J, et al. Recent Advances in Multi-target Drugs Targeting Protein Kinases and Histone Deacetylases in Cancer Therapy[J]. *Curr Med Chem*, 2020,27(42):7264-7288. DOI: 10.2174/0929867327666200102115720.
6. Zhang J, Dang F, Ren J, et al. Biochemical Aspects of PD-L1 Regulation in Cancer Immunotherapy[J]. *Trends in Biochemical Sciences*, 2018,43(12):1014-1032. DOI: <https://doi.org/10.1016/j.tibs.2018.09.004>.
7. Finn R S, Qin S, Ikeda M, et al. Atezolizumab plus Bevacizumab in Unresectable Hepatocellular Carcinoma[J]. *N Engl J Med*, 2020,382(20):1894-1905. DOI: 10.1056/NEJMoa1915745.
8. Champiat S, Ferrara R, Massard C, et al. Hyperprogressive disease: recognizing a novel pattern to improve patient management[J]. *Nat Rev Clin Oncol*, 2018,15(12):748-762. DOI: 10.1038/s41571-018-0111-2.

9. Scheiner B, Kirstein M M, Hucke F, et al. Programmed cell death protein-1 (PD-1)-targeted immunotherapy in advanced hepatocellular carcinoma: efficacy and safety data from an international multicentre real-world cohort[J]. *Aliment Pharmacol Ther*, 2019,49(10):1323-1333. DOI: 10.1111/apt.15245.
10. Gorgoulis V, Adams P D, Alimonti A, et al. Cellular Senescence: Defining a Path Forward[J]. *Cell*, 2019,179(4):813-827. DOI: 10.1016/j.cell.2019.10.005.
11. Campisi J. Aging, cellular senescence, and cancer[J]. *Annu Rev Physiol*, 2013,75:685-705. DOI: 10.1146/annurev-physiol-030212-183653.
12. Hernandez-Segura A, Nehme J, Demaria M. Hallmarks of Cellular Senescence[J]. *Trends Cell Biol*, 2018,28(6):436-453. DOI: 10.1016/j.tcb.2018.02.001.
13. Demaria M, O'Leary M N, Chang J, et al. Cellular Senescence Promotes Adverse Effects of Chemotherapy and Cancer Relapse[J]. *Cancer Discov*, 2017,7(2):165-176. DOI: 10.1158/2159-8290.CD-16-0241.
14. Lasry A, Ben-Neriah Y. Senescence-associated inflammatory responses: aging and cancer perspectives[J]. *Trends Immunol*, 2015,36(4):217-228. DOI: 10.1016/j.it.2015.02.009.
15. Coppé J P, Desprez P Y, Krtolica A, et al. The senescence-associated secretory phenotype: the dark side of tumor suppression[J]. *Annu Rev Pathol*, 2010,5:99-118. DOI: 10.1146/annurev-pathol-121808-102144.
16. Liu X, Hartman C L, Li L, et al. Reprogramming lipid metabolism prevents effector T cell senescence and enhances tumor immunotherapy[J]. *Sci Transl Med*, 2021,13(587). DOI: 10.1126/scitranslmed.aaz6314.
17. Choi Y W, Kim Y H, Oh S Y, et al. Senescent Tumor Cells Build a Cytokine Shield in Colorectal Cancer[J]. *Adv Sci (Weinh)*, 2021,8(4):2002497. DOI: 10.1002/advs.202002497.
18. Schneider J L, Rowe J H, Garcia-de-Alba C, et al. The aging lung: Physiology, disease, and immunity[J]. *Cell*, 2021,184(8):1990-2019. DOI: 10.1016/j.cell.2021.03.005.
19. Eggert T, Wolter K, Ji J, et al. Distinct Functions of Senescence-Associated Immune Responses in Liver Tumor Surveillance and Tumor Progression[J]. *Cancer Cell*, 2016,30(4):533-547. DOI: 10.1016/j.ccell.2016.09.003.
20. Hwang Y J, Lee Y, Park H, et al. Prognostic significance of viable tumor size measurement in hepatocellular carcinomas after preoperative locoregional treatment[J]. *J Pathol Transl Med*, 2021,55(5):338-348. DOI: 10.4132/jptm.2021.07.26.
21. Ingles G A, Au L, Mason R, et al. Building on the anti-PD1/PD-L1 backbone: combination immunotherapy for cancer[J]. *Expert Opin Investig Drugs*, 2019,28(8):695-708. DOI: 10.1080/13543784.2019.1649657.
22. Finkelmeier F, Waidmann O, Trojan J. Nivolumab for the treatment of hepatocellular carcinoma[J]. *Expert Rev Anticancer Ther*, 2018,18(12):1169-1175. DOI: 10.1080/14737140.2018.1535315.
23. Chibaya L, Snyder J, Ruscetti M. Senescence and the tumor-immune landscape: Implications for cancer immunotherapy[J]. *Seminars in Cancer Biology*, 2022. DOI:

<https://doi.org/10.1016/j.semcancer.2022.02.005>.

24. Lopes-Paciencia S, Saint-Germain E, Rowell M C, et al. The senescence-associated secretory phenotype and its regulation[J]. *Cytokine*, 2019,117:15-22. DOI: 10.1016/j.cyto.2019.01.013.
25. Coppé J P, Desprez P Y, Krtolica A, et al. The senescence-associated secretory phenotype: the dark side of tumor suppression[J]. *Annu Rev Pathol*, 2010,5:99-118. DOI: 10.1146/annurev-pathol-121808-102144.
26. Basisty N, Kale A, Jeon O H, et al. A proteomic atlas of senescence-associated secretomes for aging biomarker development[J]. *PLoS Biol*, 2020,18(1):e3000599. DOI: 10.1371/journal.pbio.3000599.
27. Li Y, Zhu Z, Zhang S, et al. ShRNA-targeted centromere protein A inhibits hepatocellular carcinoma growth[J]. *PLoS One*, 2011,6(3):e17794. DOI: 10.1371/journal.pone.0017794.
28. Shabangu C S, Siphepho P Y, Li C Y, et al. The Persistence of Hepatitis C Virus Infection in Hepatocytes Promotes Hepatocellular Carcinoma Progression by Pro-Inflammatory Interleukin-8 Expression[J]. *Biomedicines*, 2021,9(10). DOI: 10.3390/biomedicines9101446.
29. Bae A N, Jung S J, Lee J H, et al. Clinical Value of EZH2 in Hepatocellular Carcinoma and Its Potential for Target Therapy[J]. *Medicina (Kaunas)*, 2022,58(2). DOI: 10.3390/medicina58020155.
30. Lu M, Lu L, Dong Q, et al. Elevated G6PD expression contributes to migration and invasion of hepatocellular carcinoma cells by inducing epithelial-mesenchymal transition[J]. *Acta Biochim Biophys Sin (Shanghai)*, 2018,50(4):370-380. DOI: 10.1093/abbs/gmy009.
31. Sugiura A, Rathmell J C. Metabolic Barriers to T Cell Function in Tumors[J]. *J Immunol*, 2018,200(2):400-407. DOI: 10.4049/jimmunol.1701041.
32. Lim A R, Rathmell W K, Rathmell J C. The tumor microenvironment as a metabolic barrier to effector T cells and immunotherapy[J]. *Elife*, 2020,9. DOI: 10.7554/eLife.55185.

Figures

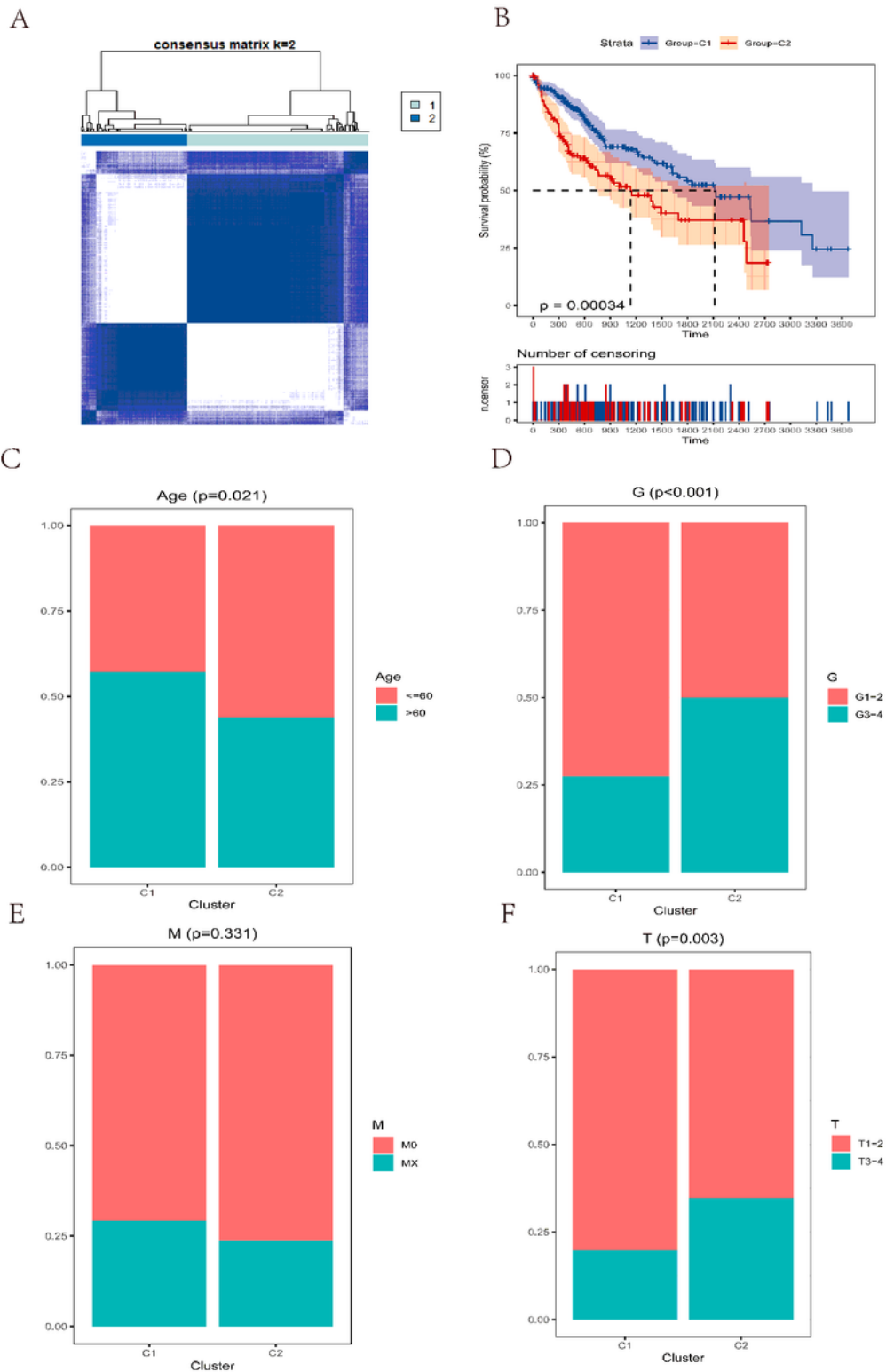


Figure 1

Clustering of HCC patients and the relationship of each clustering result with clinical characteristics and survival. (Figure 1A) Clustering of 365 HCC patients into Cluster1(C1) and Cluster2(C2) based on 279 cellular senescence gene expression;(Figure 1B) The difference between C1 and C2 in survival.(Figure 1C- Figure 1F) Relationship between C1 and C2 and clinical characteristics including age(Figure 1C), G grade(Figure 1D), M stage(Figure 1E) and T stage(Figure 1F).

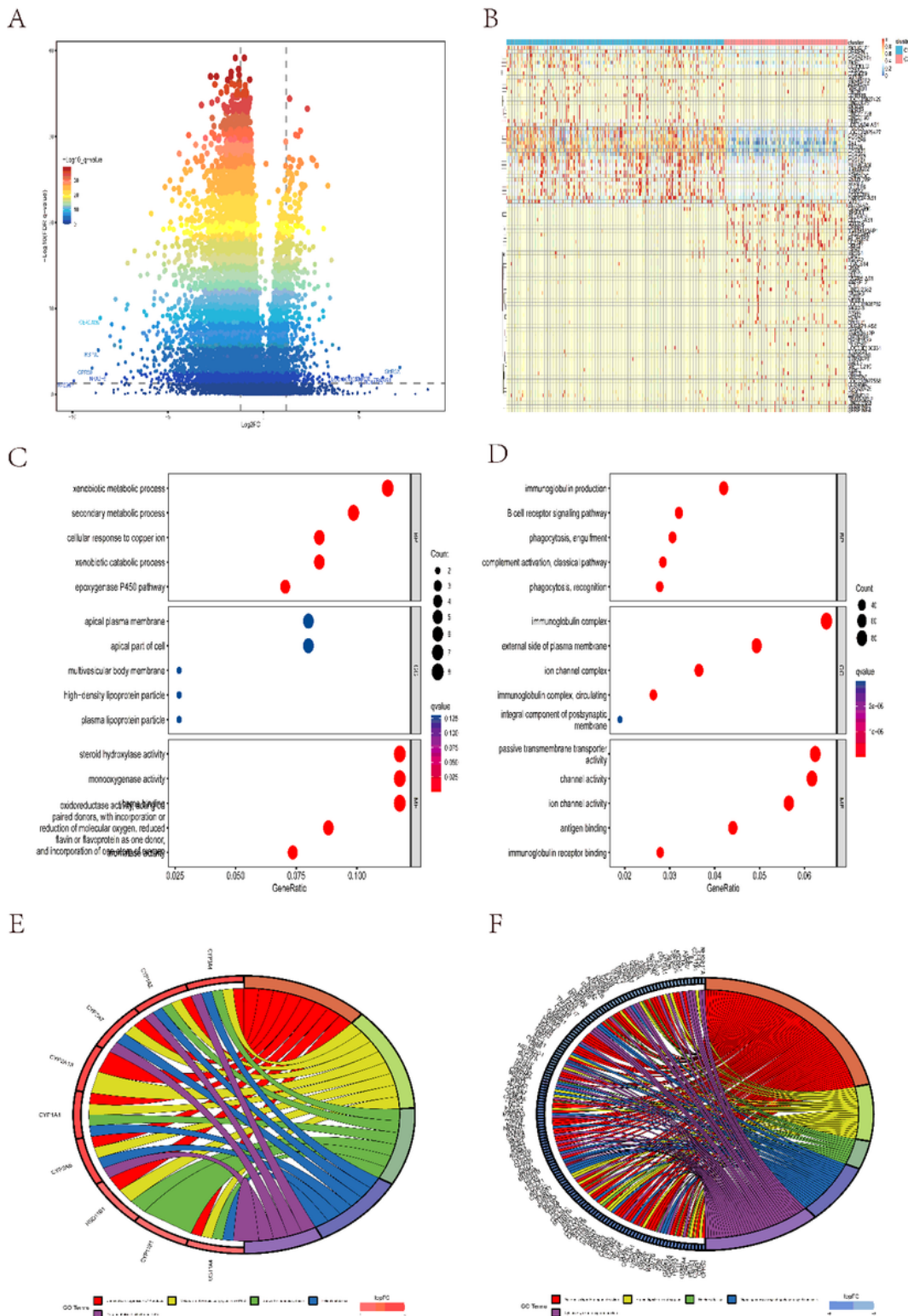


Figure 2

The differential genes between C1 and C2 and the pathways enriched by the differential genes.(Figure 2A- Figure 2B) Volcano(Figure 2A) and heatmaps(Figure 2B) of the differential genes between C1 and C2; (Figure 2C- Figure 2E) GO(Figure 2C)and KEGG(Figure 2E) enrichment analysis of upregulated genes in C1. (Figure 2D- Figure 2F) GO(Figure 2D)and KEGG(Figure 2F) enrichment analysis of upregulated genes in C2.

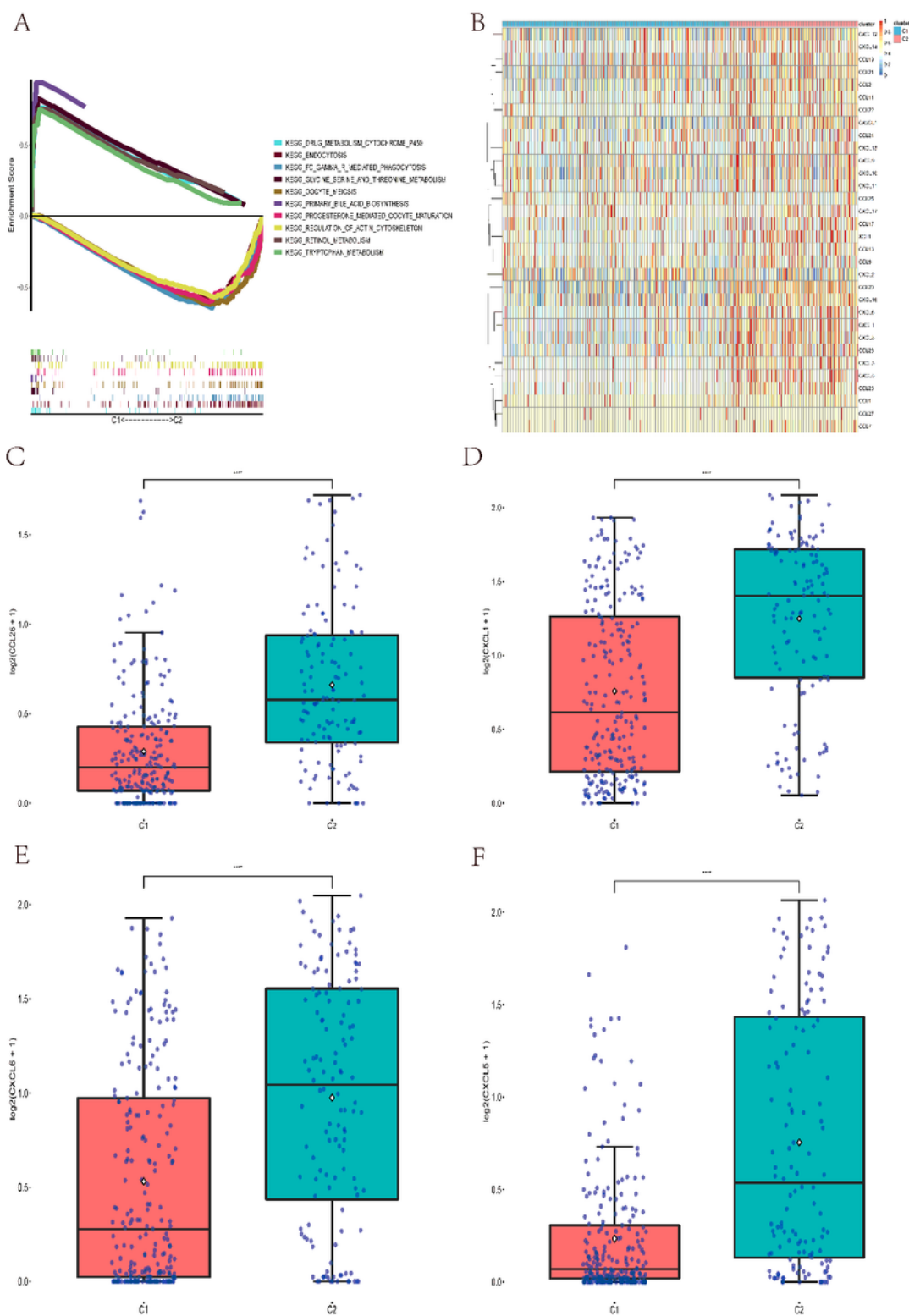


Figure 3

Results of GSEA enrichment analysis and differences in energy metabolism-related gene expression between C1 and C2.(Figure 3A) Results of GSEA enrichment analysis between C1 and C2; (Figure 3B) Heat map of energy metabolism-related gene expression between C1 and C2;(Figure 3C- Figure 3F) Boxplot of energy metabolism-related gene expression between C1 and C2.

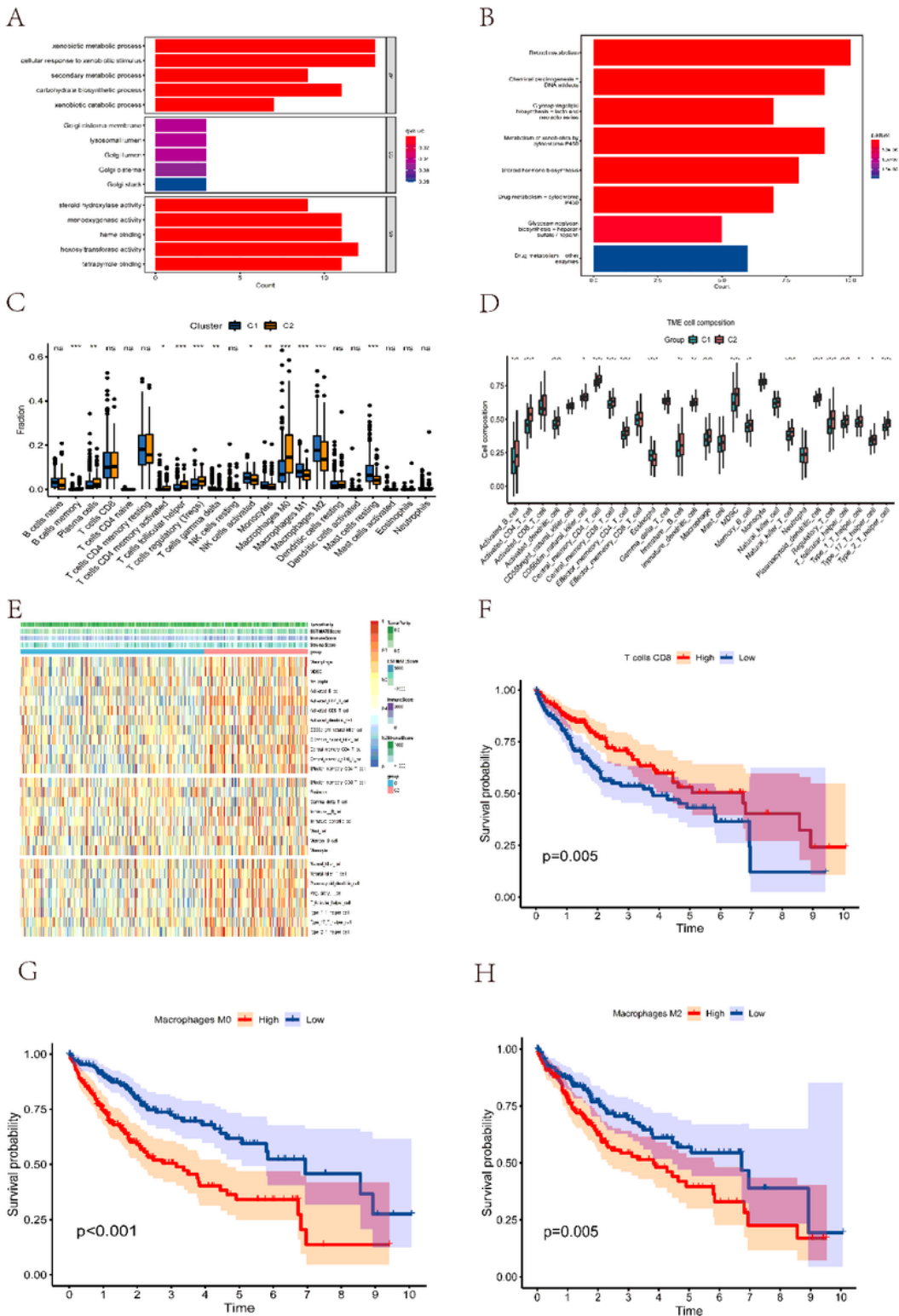


Figure 5

Signaling pathways for differential chemokine enrichment between C1 and C2 and differences in immune infiltration. (Figure 5A- Figure 5B) Signaling pathway for differential chemokine enrichment between C1 and C2; (Figure 5C- Figure 5E) Boxplot and heatmaps of the variation between C1 and C2 in immune cells and immune-related pathways; (Figure 5F- Figure 5H) Effect of differences in immune cell infiltration on survival.

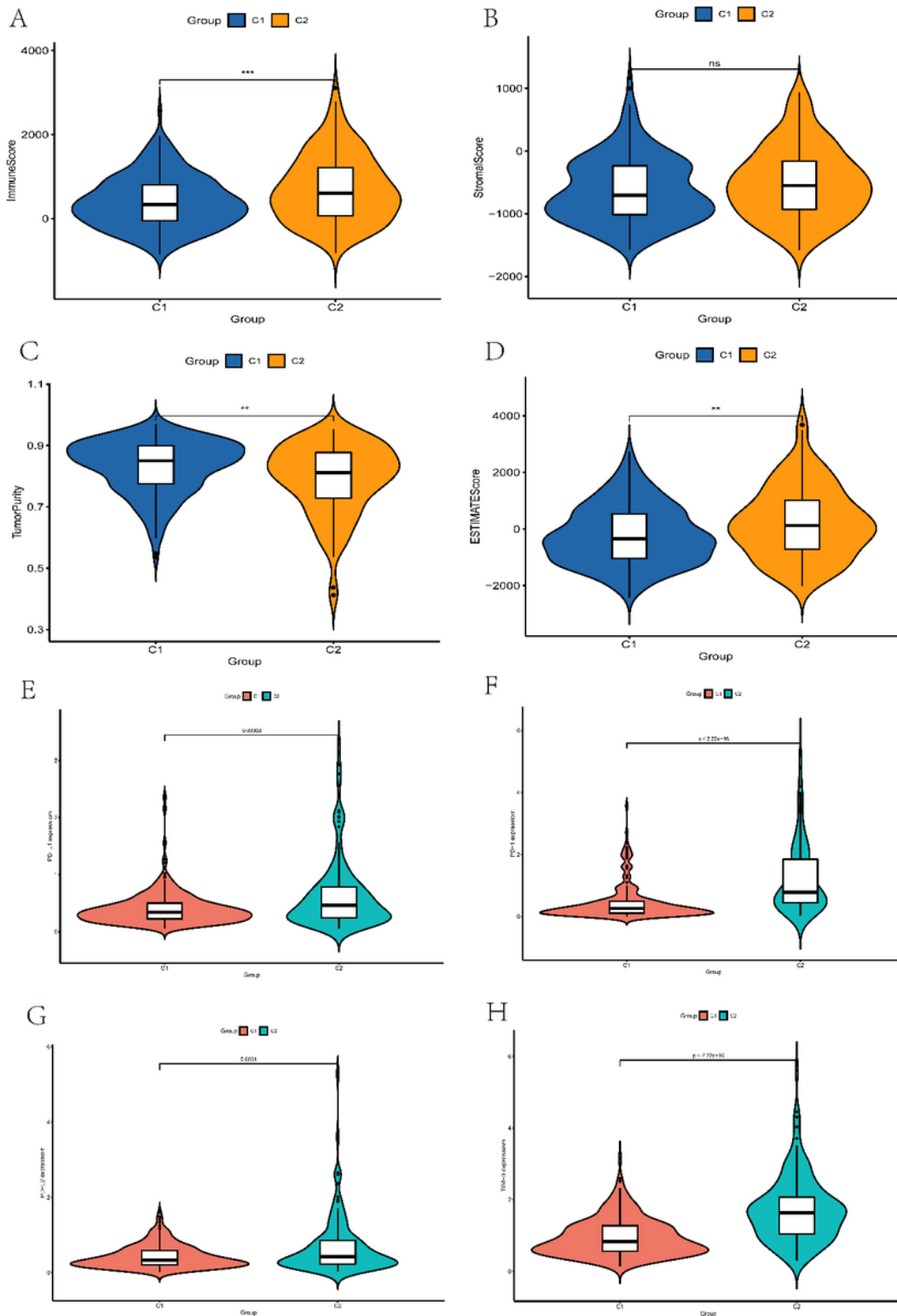


Figure 6

Differences in immune infiltration scores and immune checkpoint-associated gene expression between C1 and C2;(Figure 6A- Figure 6D) Differences between C1 and C2 in StromalScore, ImmuneScore, ESTIMATEScore, TumorPurity.(Figure 6E- Figure 6H) Differential expression between C1 and C2 in immune checkpoint-related genes including PD-L1(Figure 6E), PD-1(Figure 6F), PD-L2(Figure 6G),TIM-3(Figure 6H).

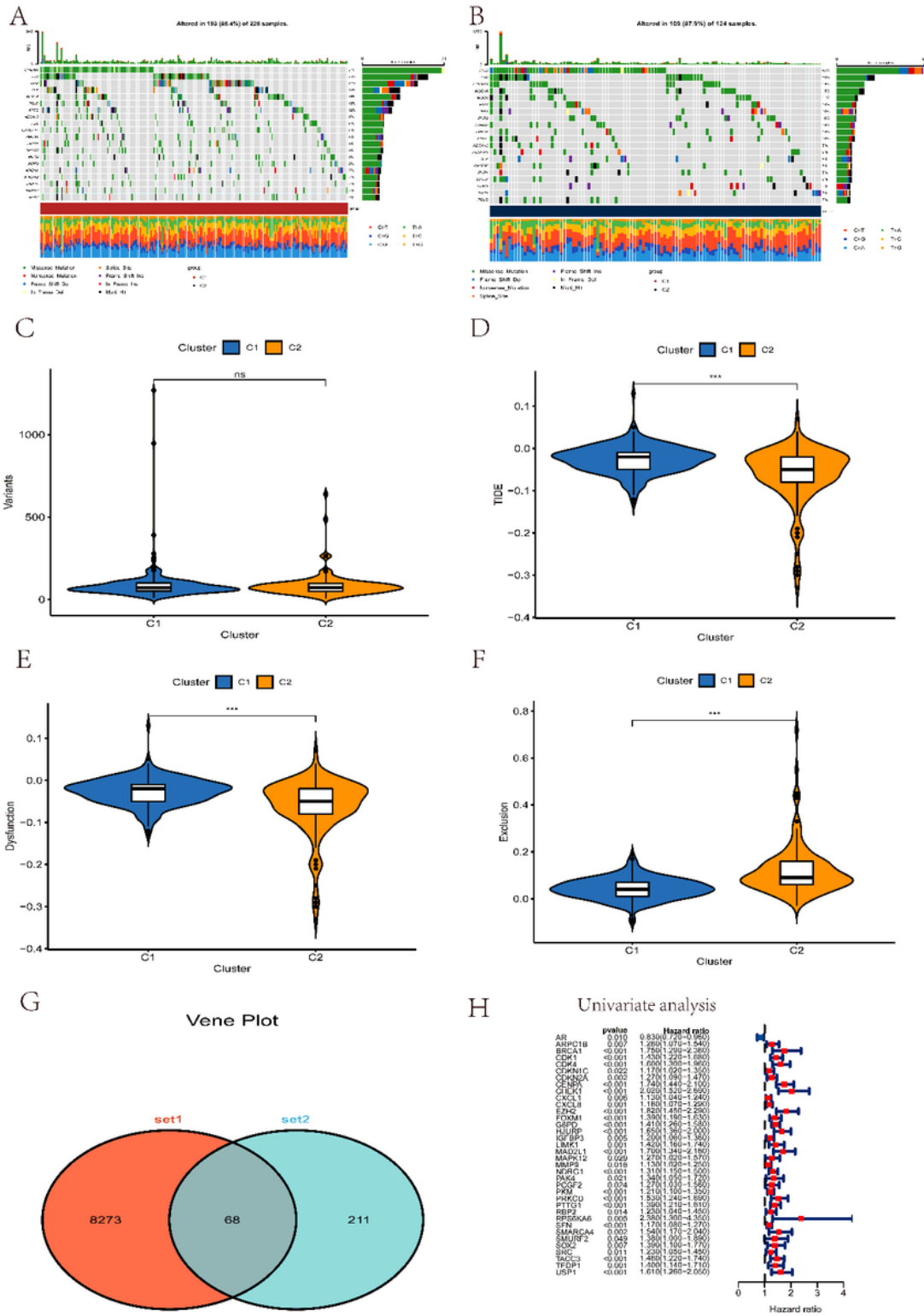


Figure 7

Differences between C1 and C2 in somatic mutations, tumor mutation borden(TMB), and TIDE scores.(Figure 7A- Figure 7B) Differences between C1 and C2 in somatic mutations;(Figure 7C) Differences between C1 and C2 in tumor mutation borden(TMB);(Figure 7D- Figure 7F) Boxplot of the difference in TIDE scores between C1 and C2;(Figure 7G) Venndiagram of the intersection of differential genes and

cellular senescence-associated genes;(Figure 7H) Results of univariate analysis of differential cellular senescence-associated genes.

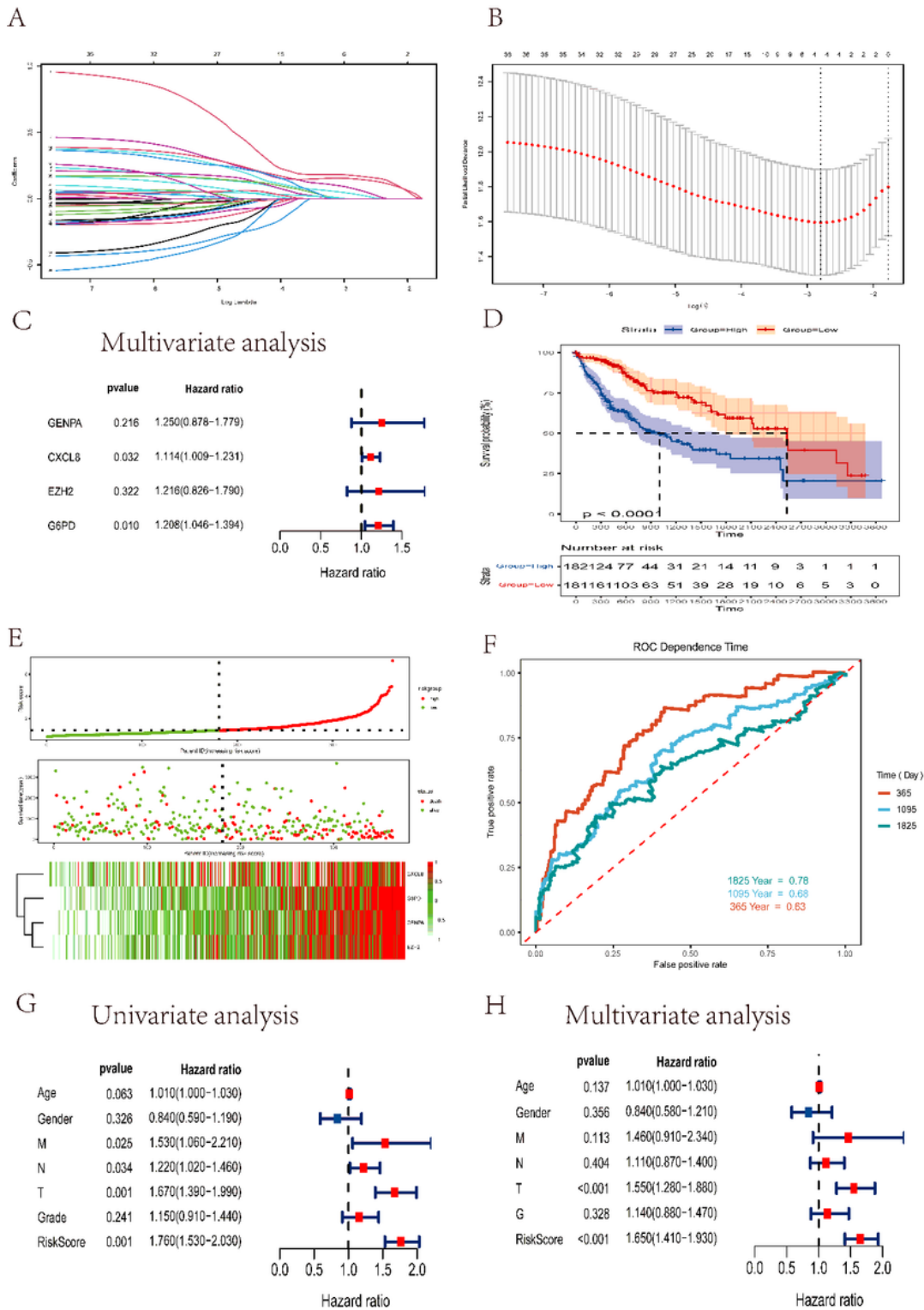


Figure 8

Construction and validation of risk scoring models.(Figure 8A- Figure 8B) LASSO regression analysis to screen the optimal number of variables;(Figure 8C) Multifactorial analysis to screen for independent risk factors affecting prognosis;(Figure 8D) Differences between high and low risk groups in survival;(Figure 8E) Relationship between risk score and survival status of HCC patients;(Figure 8F) ROC curves of risk scores for predicting 1-, 3-, and 5-year survival in HCC patients;(Figure 8G- Figure 8H) Results of univariate and multifactorial analyses of risk scores and clinical characteristics.

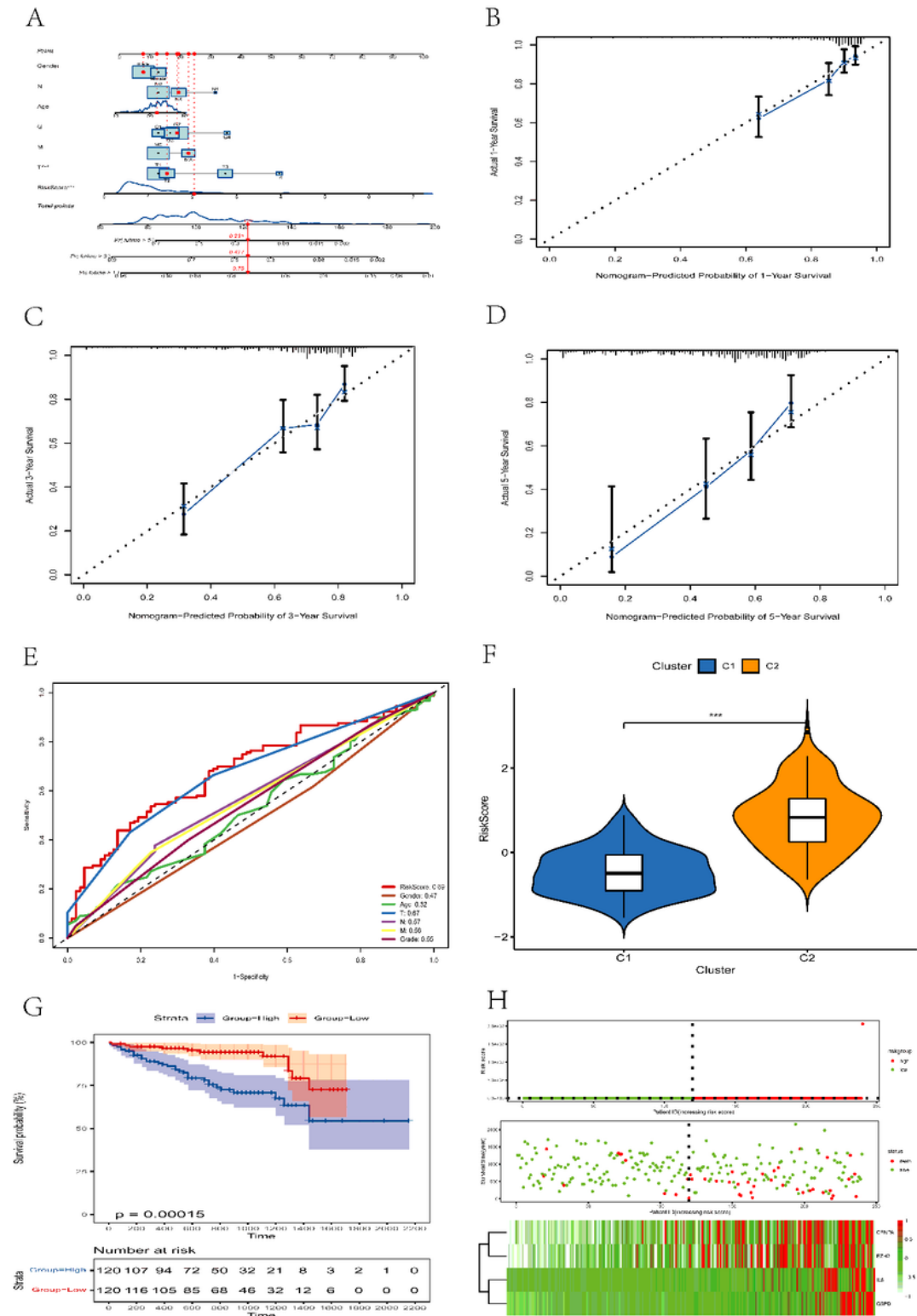


Figure 9

Clinical prediction models constructed from risk scores and clinical characteristics and validation of the models with external data. (A) Clinical prediction models constructed from risk scores and clinical characteristics; (B-D) Predictive efficacy of predictive models for 1-, 3-, and 5-year survival of HCC patients; (E) Risk scores have better diagnostic value compared to other clinical features; (F) Relationship between risk scores and C1 and C2; (G-H) External data confirm that risk scores are a valid response to patient survival.